Evidence that Chinese white olive (Canarium album(Lour.) DC.) fruits are solids of revolution

Reference:
Wang Lin, Shi Peijian, Chen Long, Gielis Johan, Niklas Karl J..- Evidence that Chinese white olive (Canarium album(Lour.) DC.) fruits are solids of revolution
Botany letters / Société botanique de France - ISSN 2381-8115 - (2023), p. 1-7
Full text (Publisher's DOI): https://doi.org/10.1080/23818107.2023.2238020
To cite this reference: https://hdl.handle.net/10067/1980010151162165141

Evidence that Chinese white olive (*Canarium album* (Lour.) DC.) fruits are solids of revolution

Lin Wang[a], Peijian Shi[a], Long Chen[a], Johan Gielis[b] and Karl J. Niklas[c]

[a]Bamboo Research Institute, College of Science, Nanjing Forestry University, Nanjing, China;

[b]Department of Biosciences Engineering, University of Antwerp, Antwerp, Belgium;

[c]School of Integrative Plant Science, Cornell University, Ithaca, NY, USA

Abstract

Although many fruit geometries resemble a solid of revolution, this assumption has rarely been rigorously examined. To test this assumption, 574 fruits of *Canarium album* (Lour.) DC. which appear to have an ellipsoidal shape, were examined to determine the validity of a general avian-based egg-shape equation, referred to as the explicit Preston equation (EPE). The assumption that the *C. album* fruit geometry is a solid of revolution is tested by applying the volume formula for a solid of revolution using the EPE. The goodness of fit of the EPE was assessed using the adjusted root-mean-square error ($RMSE_{adj}$). The relationship between the observed volume (V_{obs}) of each fruit, as measured by water displacement in a graduated cylinder, and the predicted volumes (V_{pre}) based on the EPE was also evaluated using the equation V_{pre} = slope * V_{obs}. All the $RMSE_{adj}$ values were smaller than 0.05, which demonstrated the validity of the EPE based on *C. album* fruit profiles. The 95% confidence interval of the slope of V_{pre} vs. V_{obs} included 1.0, indicating that there was no significant difference between V_{pre} and V_{obs}. The data confirm that *C. album* fruits are solids of revolution. This study provides a new approach for calculating the volume and surface area of geometrically similar fruits, which can be extended to other species with similar fruit geometries to further explore the ontogeny and evolution of angiosperm reproductive organs.

Introduction

Fruits play an indispensable role in the growth and development of angiosperms and the animals that depend upon them, especially in facilitating seed dispersal through various means (Ridley 1930; van der Pijl 1982). Fleshy fruits, in particular, serve as a source of nourishment for numerous frugivorous animals, thereby promoting the dispersal of seeds (Willson 1986). This symbiotic interaction between plants and animal dispersers has affected the evolutionary trade- off between seed and fruit size as rewards for dispersers (Edwards 2006). However, fruit traits, such as shape, size, color, scent, and texture can significantly affect the food choice of frugivores (Mazer and Wheelwright 1993; Willson 1994; Fuentes 2000; Charles-Dominique 2001; Whitney 2005; Edwards 2006; Cazetta et al. 2012; Hodgkison et al. 2013), and thus affect the outcome of seed dispersal.

Through extended periods of evolution, fleshy fruits have displayed remarkable diversity in their traits (van der Pijl 1982). In fact, certain fruit traits are commonly utilized as indicators to categorize various types of seed dispersal by animals (van der Pijl 1982; Janson 1992), which may be associated with the strong genetic component of fruit traits (Dossett et al. 2008). The investigation of fruit traits could therefore offer valuable insight into the underlying mechanisms of the evolution of plant morphology and reproductive biology.

In recent decades, fruit traits, especially size and shape, have become a major focus of interest for biologists. Size is one of the most commonly reported traits used by frugivores to select among conspecific fruits (Jordano 1987; Herrera 1988). Studies have verified that larger frugivores tend to consume larger fruits, whereas smaller frugivores tend to consume smaller fruits (Burns and Lake 2009; Burns 2013). The shape as well as the size of a fruit may also determine its probability of being eaten by frugivores, as there are specific scaling relationships between fruit size and length (Mazer and Wheelwright 1993). A recent study has also suggested that fruit shape and size interact with environmental variables and can shape plant species distributions (Trethowan et al. 2022). The study of fruit traits is helpful therefore to understand the mechanisms of fruit morphology evolution and the complex interactions between fruits and their dispersers.

Despite the importance of fruit size and shape in plant ecology, many previous studies have not mathematically quantified or precisely defined these traits with sufficient rigor. Fruit mass has often been used as a reliable indicator of “size”. However, water loss can affect the measurement consistency of fruit mass, which limits to a certain degree the utility of this measurement. Fruit volume (V) and surface area (S) are somewhat more reliable predictors for fruit size than fruit fresh mass, although water loss once again can also influence V and S as well as mass but arguably to a lesser degree. However, accurately measuring V of each individual fruit can be tedious, and non- destructive methods for measuring S have not yet been proposed. A solid of revolution is a three- dimensional geometry (i.e. a fruit) obtained by rotating a curve around a straight line (i.e. the axis of revolution). If the two-dimensional (2D) profile of the three-dimensional geometry exhibits bilateral symmetry about its mid-line (i.e. the longest segment joining the two ends of its profile, which overlaps with the axis of revolution), rotating the geometry around the mid-line by an arbitrary angle does not influence its 2D projection area, and the geometry is a solid of revolution. In this case, V and S are then easily calculated when the 2D profile of the geometry can be modelled by a mathematical equation. Although the fruits of many species exhibit good geometric symmetry and appear to be solids of revolution, it remains uncertain whether these geometries conform to the equation of a solid of revolution.

The goal of this study was to investigate the geometries of the two-dimensional fruit profiles of the Chinese white olive (*Canarium album* (Lour.) DC.), which is a member of the Burseraceae family and native to tropical Asia, the Pacific islands, and tropical Africa (Mogana and Wiart 2011). The species has been utilized in China for both food and medicinal purposes, with its extracts exhibiting potent therapeutic effects against viral and bacterial infections, inflammation, and toxicity-related ailments (He et al. 2008; Xiang et al. 2010; Yang et al. 2018). Despite its pharmacological significance, little is known about the geometry of *C. album* fruits and its intraspecific morphological variation.

The geometry of the *C. album* fruit is quite similar to that of an ellipsoid, much as is the geometry of avian eggs, which suggests that its two-dimensional profile should exhibit bilateral symmetry about its mid-line (see Figure 1). The shape of avian eggs, which potentially provides insights into some fruit geometries, has been widely studied and described by various mathematical models (e.g. Preston 1953; Troscianko 2014; Biggins et al. 2018, 2022; Narushin et al. 2021; Shi et al. 2022a). Recently, Shi et al. (2023a, 2023b), proposed a re-expression of Preston's equation, which is referred to as the explicit Preston equation (EPE), to fit the side profiles of 2221 eggs of six avian species, and confirmed the hypothesis that eggs are solids of revolution. Inspired by that work, we investigated whether EPE can effectively describe the profiles of *C. album* fruits, and whether the fruit geometry can be modelled as a solid of revolution. If both are true, we can use the formulas of V and S for the solid of revolution based on a fruit's 2D shape to calculate V and S thereby non-destructively quantifying "size" rather than using fresh mass. To achieve this goal, we used a nonlinear regression protocol based on the optimization algorithm to estimate the parameter of EPE using 574 digitized fruit profiles of *C. album*.

Figure 1. A representative *C. album* fruit image

Materials and methods

Fruit sampling and photographing

A total of 574 healthy and mature *C. album* fruits were collected in the town of Baisha (26°12'36'' N, 119°4'12'' E), Fujian, China, in November 2022. A representative fruit is shown in Figure 1. Each fruit was photographed using a smartphone (Huawei Nova5Pro, Guangzhou, China), mounted on an adjustable tabletop phone mount, while placing the fruit on a metal rack to ensure that the mid-line (i.e. the line through the two endpoints on the two-dimensional fruit profile) was parallel to the desktop and the surface of the smartphone. To calibrate the deviation of the image size of each fruit from its actual size, we measured the maximum length of the fruit using a vernier caliper (0 − 150 mm, Shanghai Accurate Measuring Tools Co. Ltd., Shanghai, China; measure accuracy: 0.02 mm.).

Image processing and profile data acquisition

To obtain the planar coordinates of fruit 2D profiles, the photographs were converted into black-and-white images and saved as .bmp format using Adobe Photoshop CS2 (version 9.0; Adobe, San Jose, CA, USA). A program developed by Shi et al. (2018) and Su et al. (2019) developed in Matlab (version ≥2009a; MathWorks, Natick, MA, USA) was then used to extract the planar coordinates of each fruit profile from the corresponding .bmp black-white image.

Modeling and data fitting

The explicit Preston equation (Shi et al. 2023a, 2023b) is

$$Y = \pm b\sqrt{1-\left(\frac{X}{a}\right)^2}\left(1+c_1\left(\frac{X}{a}\right)+c_2\left(\frac{X}{a}\right)^2+c_3\left(\frac{X}{a}\right)^3\right), \quad (1)$$

where (X, Y) represents an arbitrary coordinate point on a fruit profile, and a, b, c_1, c_2, and c_3 are constants to be estimated. Among these, a and b denote half of the fruit length and approximately half of the fruit maximum width, respectively. The upper and lower parts of the fruit profile correspond to positive and negative signs in Equation (1), respectively. The function "fitEPE" in the package "biogeom" (version 1.3.5) (Shi et al. 2022b) in R (version 4.2.1) (R Core Team 2022) was used to estimate the numerical values of a, b, c_1, c_2, and c_3. The Nelder-Mead optimization method (Nelder and Mead 1965) was used to minimize the residual sum of squares (RSS) between the observed and predicted Y-values of *C. album* fruit profiles.

Testing the solid of revolution hypothesis

Assuming that the *C. album* fruit can be modelled as a solid of revolution, the predicted V and S of a fruit can be estimated by using the volume and surface area formulas of its solid of revolution (Narushin et al. 2022; Shi et al. 2023b), which is based on Equation (1). The predicted V and S of each fruit was calculated using the formulas.

$$\begin{aligned} V &= \int_{-a}^{a} \pi Y^2 dX \\ &= \frac{4}{315}\pi a b^2\left(105+21c_1^2+42c_2+9c_2^2+18c_1c_3+5c_3^2\right), \end{aligned} \quad (2)$$

and

$$S = \int_{-a}^{a} 2\pi Y\sqrt{1+\left(\frac{dY}{dX}\right)^2}dX, \quad (3)$$

where d represents the differential sign. In practice, it is fairly difficult to measure the S of any object that is not a simple geometry such as a cube, sphere, or ellipsoid. However, the V of even a complex geometry can be measured empirically by submerging an object under water in a graduated cylinder and recording the fluid's displacement. To compare the predicted V of a fruit with its observed V, we measured V by submerging each fruit in water in a 250 mL graduated cylinder with a diameter of 4 cm and reading the observed volume of displaced water.

In order to compare empirically measured fruit volumes with predicted volumes, Equation (2) can be re-written as

$$V = \frac{4}{3}\pi ab^2\left(1 + \frac{1}{5}c_1^2 + \frac{2}{5}c_2 + \frac{3}{35}c_2^2 + \frac{6}{35}c_1c_3 + \frac{1}{21}c_3^2\right). \tag{4}$$

Note that the volume of – a standard ellipsoid V_e (i.e. the solid of revolution obtained by rotating an ellipse around the *x*-axis with the semi-major and semi-minor axes *a* and *b*, respectively) is equal to

$$V_e = \frac{4}{3}\pi ab^2. \tag{5}$$

The item after $4/3\pi ab^2$ on the right-hand side of Equation (4) is defined as the ellipsoid index (EI), i.e.

$$\mathrm{EI} = 1 + \frac{1}{5}c_1^2 + \frac{2}{5}c_2 + \frac{3}{35}c_2^2 + \frac{6}{35}c_1c_3 + \frac{1}{21}c_3^2. \tag{6}$$

EI serves as a measure of the degree to which the geometry of a particular fruit approximates a regular ellipsoid as described by Equation (5). If the EI of a fruit converges onto 1, the fruit is more approximately considered a regular ellipsoid.

Data analysis

The adjusted root-mean-square error ($\mathrm{RMSE_{adj}}$) was calculated to assess the goodness of fit between observed and predicted data sets (Shi et al. 2023a, 2023b). It represents the proportion of the mean deviation between the observed and predicted *Y* values (i.e. RMSE) to one half of a fruit's maximum width:

$$\mathrm{RMSE_{adj}} = \sqrt{\frac{1}{N}\sum_{i=1}^{N}\left(Y_i - \hat{Y}_i\right)^2} \Big/ \left(\frac{W}{2}\right), \tag{7}$$

where *N* represents the number of data points on a fruit profile; Y_i and $\hat{Y}_i$ represent the observed and predicted *Y* values, respectively; and *W* represents the fruit maximum width. As a rule of thumb, an $\mathrm{RMSE_{adj}}$ value <0.05 usually indicates a good fit, i.e. the mean absolute deviation between the observed and predicted distances from the data points on a fruit profile to the mid-line of the profile does not exceed 5% of the half of the fruit maximum width.

The relationship between the observed volumes (V_{obs}) of fruits, as measured by water displacements in a graduated cylinder, and the predicted volumes (V_{pre}) of fruits calculated by EPE was evaluated using reduced major axis (RMA) regression protocols (Niklas 1994; Quinn and Keough 2002) to fit the equation V_{pre} = slope*V_{obs}. The bootstrap percentile method (Efron and Tibshirani 1993; Sandhu et al. 2011) was used to calculate the 95% confidence interval (CI) of the regression slope. If the 95% CI of the slope includes unity, there is no significant difference between V_{pre} and V_{obs}, indicating that *C. album* fruits can be treated as solids of revolution. Equation (3) was also used to predict *S* of each fruit and fitted the scaling relationship between the predicted surface area and volume for the 574 fruits using RMA regression protocols.

To estimate EI in Equation (6), linear regression protocols with no intercept were performed between the predicted volume of the fruit and $4/3\pi ab^2$ (where *a* and *b* are constants estimated by Equation (1)) using RMA regression protocols. Once again, if the 95% CI of the slope calculated using the bootstrap percentile method includes unity, there is no significant difference between the predicted volume of the fruit and $4/3\pi ab^2$, which means that the *C. album* fruits can be treated as standard ellipsoids.

Results

The adjusted RMSE ($RMSE_{adj}$) values for all fruit profiles predicted by Equation (7) fell within the range of 0.008 to 0.049, which were all smaller than 0.05 (as shown in Figure 2). This result was interpreted to indicate that the explicit Preston equation (EPE) is a valid method for accurately depicting the profiles of *C. album* fruits. Figure 3 provides examples of the curves of the observed and predicted profiles of one fruit among the 574 fruits, which graphically provides the validity of EPE in describing fruit profiles.

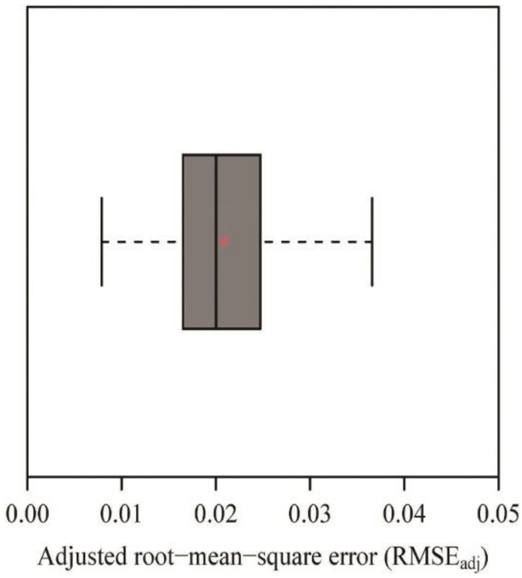

Figure 2. Box plot of the adjusted root-mean-square error ($RMSE_{adj}$) calculated by Equation (7) calculated by Equation (7) between observed and predicted *Y*-values. The vertical solid line represents the median, and the asterisk within the box represents the mean.

The zero-intercept linear regression analysis between the observed and predicted fruit volumes revealed that the 95% CI of the slope included unity (Figure 4), which indicated that there was no significant difference between the observed and predicted volumes. This finding supported the assumption that the fruits of *C. album* can be treated as solids of revolution. There was a strong scaling relationship between fruit surface area and volume ($r^2 = 0.99$) on a log-log scale (Figure 5). The numerical value of the slope was approximate to 2/3, i.e. *S* scales as the 2/3– power of *V* on a log-log scale.

In contrast, linear regression analysis between the predicted *V* using EPE and the predicted *V* using $4/3\pi ab^2$ (i.e. the ellipsoid prediction) revealed that the 95% confidence interval of the slope did not include unity (Figure 6), indicating that the fruit volumes significantly differed from those predicted if fruits were truly ellipsoid, i.e. the geometry of fruits cannot be regarded as a standard ellipsoid.

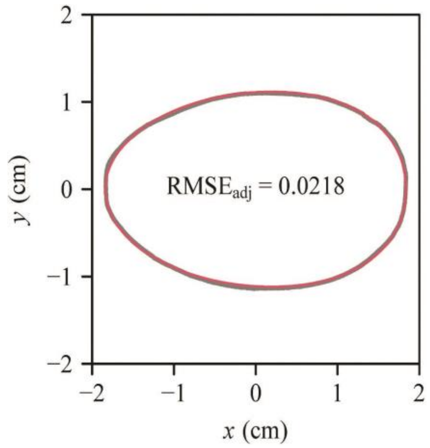

Figure 3. The observed (gray) and the predicted (red) boundary geometries of a representative fruit (see Figure 1) simulated using Equation (1). RMSE$_{adj}$ represents the adjusted root- mean-square error calculated using Equation (7).

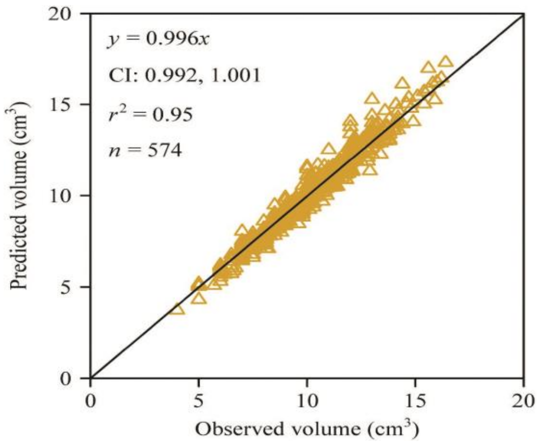

Figure 4. Results of linear regression with no intercept between the observed and predicted fruit volumes. Here, *y* denotes the predicted volume calculated using Equation (2), and *x* denotes the observed volume using the water displacement graduated cylinder method; CI represents the 95% confidence interval of the slope; r^2 is the coefficient of determination which reflects the goodness of fit; *n* is the sample size (i.e. the number of fruits).

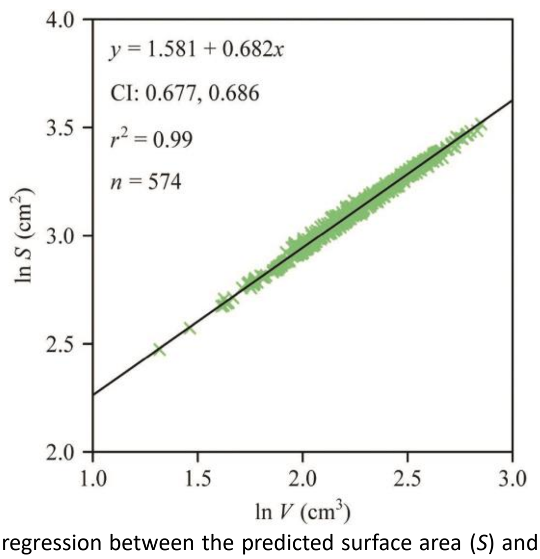

Figure 5. Results of linear regression between the predicted surface area (*S*) and volume (*V*) of fruits plotted on a log-log scale. Here, *y* denotes the predicted *S* calculated using Equation (3) on a log scale, and *x* denotes the predicted *V* calculated using Equation (2) on a log scale; CI represents the 95% confidence interval of the slope; r^2 is the coefficient of determination; *n* is the sample size (i.e. the number of fruits).

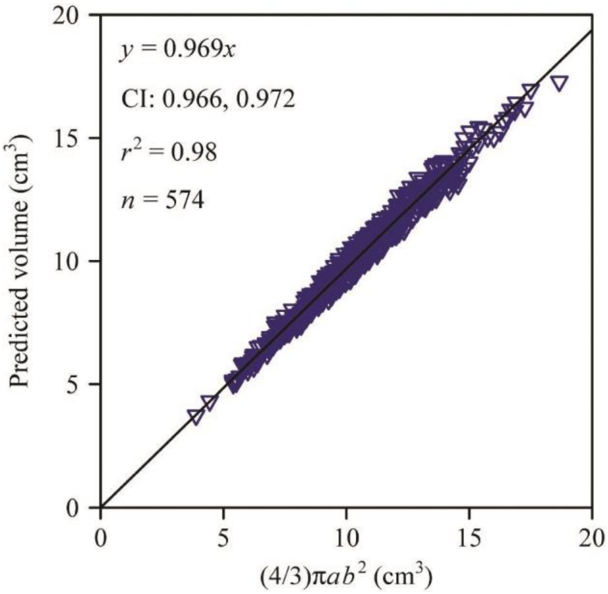

Figure 6. Results of linear regression with no intercept between the predicted *V* (based on the volume formula of a solid of revolution) and the *V* based on the standard ellipsoid fruit hypothesis (calculated using Equation (5)). Here, *y* denotes the predicted *V* calculated using Equation (2), and *x* denotes $4/3\pi ab^2$ (where *a*, *b* are constants estimated using Equation (1)); CI represents the 95% confidence interval of the slope (i.e. EI in Equation (6)); r^2 is the coefficient of determination; *n* is the sample size (i.e. the number of fruits).

Discussion

Reliability and validity of EPE in modeling C. album fruit geometry

Preston's equation, originally proposed to model avian eggs using an elliptic parametric equation (Preston 1953), has been widely adopted to fit the 2D profiles of diverse avian eggs. Multiple linear regression methods have been employed to estimate the parameters in modeling planar egg-shapes using Preston's equation or its simplified versions, leading to good statistical fits between observed and predicted values, but under the assumption of perfect bilateral symmetry (Biggins et al. 2022), which may not hold true for many organic structures, including *C. album* fruits.

To overcome this limitation, Shi et al. (2023a) proposed a nonlinear optimization algorithm to estimate the parameters of the explicit Preston equation, which considers the asymmetry of fruit profiles. In the present study, we used the method of Shi et al. (2023a) to fit the profiles of *C. album* fruits in a manner similar to treating avian eggs in prior studies. It is apparent that measurement errors in photographing fruits can decrease the prediction accuracy. For example, placement errors would occur if the mid-line of a fruit was not parallel to a desktop and the surface of a smartphone. Additionally, the surface of *C. album* fruit is usually not sufficiently smooth and its three- dimensional (3D) geometry is also not as regular as that of an egg and can be deformed by a variety of abiotic and biotic factors (Bajcz 2014), resulting in profiles that are not perfectly bilaterally symmetrical. Nevertheless, apart from the traditional multiple linear regression method, the nonlinear optimization method (Shi et al. 2023a, 2023b) can sufficiently cope with fruit profile asymmetries. This assertion is based on the $RMSE_{adj}$ values reported here, all of which are smaller than 0.05, thereby verifying the reliability and validity of the EPE in describing the natural profiles of *C. album* fruits.

Comparison between the geometry of C. album fruits and the standard ellipsoid

The results of the linear regression analysis between the predicted volume of fruit using the EPE and using the formula for a standard ellipsoid (i.e. $4/3\pi ab^2$, where a and b are constants estimated by Equation (1)) demonstrate that predicted fruit volumes are significantly different from those based on the supposition that fruits are ellipsoids, i.e. olive fruits cannot be treated as regular ellipsoids. Nevertheless, there is a strong linear correlation between the predicted volume using the EPE and the ellipsoid equation $4/3\pi ab^2$, i.e. $r^2 = 0.98$ (Figure 6). Thus, Equation (5) can be considered as a modified formula for calculating fruit volume if fruit shape approximately conforms to that of a regular ellipsoid, and the EI in Equation (6) can be used as a correction coefficient that reflects the differences between actual fruit shape and that of a standard ellipsoid. The EI might also be useful in describing the degree of environmental stress on *C. album* fruits because the irregularity of fruit geometry tends to be related to environmental stress. In general, the greater the environmental stress experienced by a fruit during growth, the greater the fruit irregularity in shape. The measure for the deviation of fruit geometry from a standard ellipsoid (i.e. EI) therefore provides insights into the evolution of plant morphology and to a certain degree angiosperm reproductive biology.

Conclusions

This study supports the validity of the explicit Preston equation (EPE) for describing the 2D profiles of *Canarium album* fruits based on the goodness of fit between predicted and observed fruit volumes. The results also indicate that the *C. album* fruit can be accurately modelled as a solid of revolution, which enables the development of a more efficient method for calculating fruit volume and surface area. By comparing fruit 3D geometry with that of a regular ellipsoid, we also introduce the ellipsoid index (i.e. EI in Equation (6)) to quantify the extent to which a fruit approximates a standard ellipsoid that can in turn potentially reflect the influence of environmental stress on fruit growth and development. The volume and surface area calculation method presented here is potentially transferable to other plant species that share similar fruit geometries and can be helpful in studying fruit ontogeny and making interspecific comparisons of fruit geometries for taxonomic and evolutionary investigations.

References

Bajcz AW. 2014. Reproductive ecophysiology of *Rubus occidentalis* in southeastern Michigan II. Variation in fruit characteristics relates to light and soil conditions. Rhodora. 116(967):267–282. doi: 10.3119/13-18 Biggins JD, Montgomerie R, Thompson JE, Birkhead TR. 2022. Preston's universal formula for avian egg shape. Ornithology. 139(4):1–8. doi: 10.1093/ornithology/ ukac028

Biggins JD, Thompson JE, Birkhead TR. 2018. Accurately quantifying the shape of birds' eggs. Ecol Evol. 8 (19):9728–9738. doi: 10.1002/ece3.4412

Burns KC. 2013. What causes size coupling in fruit–frugivore interaction webs? Ecology. 94(2):295–300. doi: 10. 1890/12-1161.1.

Burns KC, Lake B. 2009. Fruit–frugivore interactions in two southern hemisphere forests: allometry, phylogeny and body size. Oikos. 118(12):1901–1907. doi: 10.1111/j.1600- 0706.2009.17661.x.

Cazetta E, Galetti M, Rezende EL, Schaefer HM. 2012. On the reliability of visual communication in vertebrate-dispersed fruits. J Ecol. 100(1):277–286. doi: 10.1111/j.1365-2745.2011.01901.x.

Charles-Dominique P. 2001. Relationships between seed dispersal and behavioural ecology. Dordrecht (Netherlands): Springer Netherlands. doi: 10.1007/978- 94-015-9821-7_17.

Dossett M, Lee J, Finn CE. 2008. Inheritance of phenological, vegetative, and fruit chemistry traits in black raspberry. J Amer Soc Hort Sci. 133(3):408–417. doi: 10.21273/JASHS.133.3.408.

Edwards W. 2006. Plants reward seed dispersers in proportion to their effort: the relationship between pulp mass and seed mass in vertebrate dispersed plants. Evol Ecol. 20(4):365–376. doi: 10.1007/s10682-006-0006-z.

Efron B, Tibshirani RJ. 1993. An introduction to the bootstrap. Florida: Chapman and Hall/CRC. doi: 10.1007/ 978-1-4899-4541-9.

Fuentes M. 2000. Frugivory, seed dispersal and plant community ecology. Trends Ecol Evol. 15(12):487–488. doi: 10.1016/S0169-5347(00)02031-0.

Herrera CM. 1988. The fruiting ecology of *Osyris quadripartita*: individual variation and evolutionary potential. Ecology. 69(1):233–249. doi: 10.2307/1943179.

He Z, Xia W, Chen J. 2008. Isolation and structure elucidation of phenolic compounds in Chinese olive (*Canarium album* L.) fruit. Eur Food Res Technol. 226(5):1191–1196. doi: 10.1007/s00217-007-0653-5.

Hodgkison R, Ayasse M, Häberlein C, Schulz S, Zubaid A, Mustapha WAW, Kunz TH, Kalko EKV . 2013. Fruit bats and bat fruits: the evolution of fruit scent in relation to the foraging behaviour of bats in the New and Old World tropics. Funct Ecol. 27(4):1075–1084. doi: 10.1111/1365- 2435.12101.

Janson CH. 1992. Measuring evolutionary constraints: a Markov model for phylogenetic transitions among seed dispersal syndromes. Evolution. 46(1):136–158. doi: 10.2307/2409810.

Jordano P. 1987. Avian fruit removal: effects of fruit variation, crop size, and insect damage. Ecology. 68 (6):1711–1723. doi: 10.2307/1939863.

Mazer SJ, Wheelwright NT. 1993. Fruit size and shape: allometry at different taxonomic levels in bird-dispersed plants. Evol Ecol. 7(6):556–575. doi: 10.1007/ BF01237821.

Mogana R, Wiart C. 2011. Canarium L.: A phytochemical and pharmacological review. J Pharm Res. 4 (8):2482–2489. doi: 10.4061/2011/768673.

Narushin VG, Romanov MN, Griffin DK. 2021. Egg and math: Introducing a universal formula for egg shape. Ann N Y Acad Sci. 1505(1):169–177. doi: 10.1111/nyas.14680.

Narushin VG, Romanov MN, Mishra B, Griffin DK. 2022. Mathematical progression of avian egg shape with associated area and volume determinations. Ann N Y Acad Sci. 1513(1):65–78. doi: 10.1111/nyas.14771.

Nelder JA, Mead R. 1965. A simplex method for function minimization. Comput J. 7(4):308–313. doi: 10.1093/ comjnl/7.4.308.

Niklas KJ. 1994. Plant allometry. Chicago: University of Chicago Press.

Preston FW. 1953. The shapes of birds' eggs. Auk. 70 (2):160–182. doi: 10.2307/4081145.

Quinn GP, Keough MJ. 2002. Experimental design and data analysis for biologists. Cambridge: Cambridge University Press.

R Core Team. 2022. R: a language and environment for statistical computing. Vienna (Austria): R Foundation for Statistical Computing; [accessed 2022 July 1]. https://www.R-project.org/ .

Ridley HN. 1930. The dispersal of plants throughout the world. Ashford, Kent: L. Reeve and Co., Ltd.

Sandhu HS, Shi P, Kuang X, Xue F, Ge F. 2011. Applications of the bootstrap to insect physiology. Fla Entomol. 94 (4):1036–1041. doi: 10.1653/024.094.0442.

Shi P, Chen L, Quinn BK, Yu K, Miao Q, Guo X, Lian M, Gielis J, Niklas KJ. 2023a. A simple way to calculate the volume and surface area of avian eggs. Ann N Y Acad Sci. 1524(1):118–131. doi: 10.1111/nyas.15000.

Shi P, Gielis J, Niklas KJ. 2022a. Comparison of a universal (but complex) model for avian egg shape with a simpler model. Ann N Y Acad Sci. 1514(1):34–42. doi: 10.1111/ nyas.14799.

Shi P, Gielis J, Quinn BK, Niklas KJ, Ratkowsky DA, Schrader J, Ruan H, Wang L, Niinemets Ü. 2022b. 'Biogeom': an R package for simulating and fitting natural shapes. Ann NY Acad Sci. 1516(1):123–134. doi: 10.1111/ nyas.14862.

Shi P, Ratkowsky DA, Li Y, Zhang L, Lin S, Gielis J. 2018. A general leaf area geometric formula exists for plants— evidence from the simplified gielis equation. Forests. 9 (11):714. doi: 10.3390/f9110714.

Shi P, Wang L, Quinn BK, Gielis J. 2023b. A new program to estimate the parameters of preston's equation, a general formula for describing the egg shape of birds. Symmetry. 15(1):231. doi: 10.3390/sym15010231.

Su J, Niklas KJ, Huang W, Yu X, Yang Y, Shi P. 2019. Lamina shape does not correlate with lamina surface area: an analysis based on the simplified Gielis equation. Glob Ecol Conserv. 19:e00666. doi:10.1016/j.gecco.2019. e00666.

Trethowan LA, Jennings L, Bramley G, Clark R, Dawson S, Moore A, Pearce L, Puglisi C, Riwu-Kaho M, Rosaria, et al. 2022. Environment - dependent influence of fruit size upon the distribution of the Malesian archipelagic flora. Plants

People Planet. [accessed 2023 May 1]. 10. doi: 10. 1002/ppp3.10348.

Troscianko J . 2014. A simple tool for calculating egg shape, volume and surface area from digital images. Ibis (Lond 1859). 156(4):874–878. doi: 10.1111/ibi.12177. van der Pijl L. 1982. Principles of dispersal in higher plants. New York: Springer-Verlag. doi: 10.1007/978-3-642- 87925-8.

Wang L, Shi P, Chen L, Gielis J, Niklas KJ. 2023. Data from: fruit-shape data of 574 Chinese white olives. Dryad Digital Repository. 2023 July 7. doi: 10.5061/dryad. 2547d7wwz.

Whitney KD. 2005. Linking frugivores to the dynamics of a fruit color polymorphism. Am J Bot. 92(5):859–867. doi: 10.3732/ajb.92.5.859.

Willson MF. 1986. Avian frugivory and seed dispersal in Eastern North America. In Johnston R editor. Current ornithology Vol. 2. New York (NY): Springer US. pp. 223–279. doi: 10.1007/978-1-4615-6784-4_5.

Willson MF. 1994. Fruit choices by captive American robins. Condor. 96(2):494–502. doi: 10.2307/1369331.

Xiang Z, Chen H, Jin Y, Wang G, Xiang L, Chen W. 2010. Phenolic constituents of *Canarium album*. Chem Nat Compd. 46(1):119–120. doi: 10.1007/s10600-010- 9543-3.

Yang L, Gu X, Chen J, Yang J, Tan S, Duan W. 2018. Chemical constituents from *Canarium album* Raeusch and their anti-influenza A virus activities. J Nat Med. 72 (3):808–815. doi: 10.1007/s11418-018-1208-8